Eur. J. Mineral., 35, 703–714, 2023
https://doi.org/10.5194/ejm-35-703-2023

European Journal of Mineralogy
Open Access

Batoniite, $[Al_8(OH)_{14}(H_2O)_{18}](SO_4)_5 \cdot 5H_2O$, a new mineral with the $[Al_8(OH)_{14}(H_2O)_{18}]^{10+}$ polyoxocation from the Cetine di Cotorniano Mine, Tuscany, Italy

Daniela Mauro[1,2], **Cristian Biagioni**[1,3], **Jiří Sejkora**[4], **Zdeněk Dolníček**[4], **and Radek Škoda**[5]

[1]Dipartimento di Scienze della Terra, Università di Pisa, Via Santa Maria 53, 56126 Pisa, Italy
[2]Museo di Storia Naturale, Università di Pisa, Via Roma 79, 56011 Calci, Italy
[3]Centro per l'Integrazione della Strumentazione scientifica dell'Università di Pisa (C.I.S.U.P.), Università di Pisa, Pisa, Italy
[4]Department of Mineralogy and Petrology, National Museum, Cirkusová 1740, 193 00 Prague 9, Czech Republic
[5]Department of Geological Sciences, Faculty of Science, Masaryk University, Kotlářská 2, 611 37 Brno, Czech Republic

Correspondence: Daniela Mauro (daniela.mauro@unipi.it)

Received: 21 April 2023 – Revised: 8 July 2023 – Accepted: 22 July 2023 – Published: 31 August 2023

Abstract. The new mineral batoniite, $[Al_8(OH)_{14}(H_2O)_{18}](SO_4)_5 \cdot 5H_2O$, was discovered in the Cetine di Cotorniano Mine, Chiusdino, Siena, Tuscany, Italy. It occurs as hemispherical aggregates composed of brittle tabular crystals, up to 1 mm in size, white to colorless in color, with a white streak and a vitreous to greasy luster. Batoniite is biaxial negative, with $\alpha = 1.4833(6)$, $\beta = 1.4948(6)$, $\gamma = 1.5019(5)$ (589 nm), and $2V_{(meas.)} = 71(1)^\circ$. Electron microprobe analysis, affected by the dehydration of batoniite under the chamber vacuum, gave (in wt %) the following: Al_2O_3 33.48, Fe_2O_3 0.05, SO_3 33.00, and H_2O_{calc} 44.41, total 110.94. It corresponds to the chemical formula $(Al_{7.98}Fe^{3+}_{0.01})_{\Sigma 7.99}(SO_4)_{5.01}(OH)_{13.95}(H_2O)_{18} \cdot 5H_2O$. Batoniite is triclinic, belonging to space group $P\bar{1}$, with $a = 9.1757(6)$, $b = 12.0886(9)$, $c = 20.9218(15)$ Å, $\alpha = 82.901(3)$, $\beta = 87.334(3)$, $\gamma = 86.999(2)^\circ$, $V = 2297.8(3)$ Å^3, and $Z = 2$. The crystal structure was refined to $R_1 = 0.0916$ for 8118 unique reflections with $F_o > 4\sigma(F_o)$ and 811 refined parameters and 60 restraints. Batoniite is characterized by isolated $[Al_8(OH)_{14}(H_2O)_{18}]^{10+}$ polyoxocations, H-bonded to five interstitial $(SO_4)^{2-}$ and five H_2O groups. In type material, it is associated with gypsum and a poorly crystallized Al–Fe sulfate. The crystallization of batoniite is probably due to the action of H_2SO_4 on Al-bearing rocks of Paleozoic age cropping out in the Garibaldi Tunnel, the lowest mining level of the Cetine di Cotorniano Mine.

1 Introduction

During the last 15 years, we have been involved in the study of sulfate assemblages originating from the oxidation of primary sulfide ores from Tuscany (Italy). In particular, our attention was mainly focused on the pyrite ore deposits of the Apuan Alps (northern Tuscany), where several well-crystallized sulfates were identified (e.g., Biagioni et al., 2020b), along with some new species, i.e., the phosphate sulfate mineral bohuslavite (Mauro et al., 2019; Mauro and Biagioni, 2023) and the three K–Fe^{3+} sulfates giacovazzoite, scordariite, and magnanelliite (Biagioni et al., 2019a, b, 2020a). Other results were achieved through the study of secondary phases derived from the weathering of Cu deposits hosted in ophiolitic rocks, with the finding of the new mineral species tiberiobardiite (Biagioni et al., 2018).

An interesting locality for the study of secondary sulfates is represented by the Cetine di Cotorniano Mine (province of Siena, Tuscany), which formerly exploited an Sb ore deposit hosted in silicified limestones. At the beginning of the 20th century, Manasse (1908) described melanterite and fibrofer-

rite from this locality. Later, during the 1980s, some authors reported the occurrence of several other species, e.g., ferrinatrite, jurbanite, metavoltine, rostite, sideronatrite, tamarugite, tschermigite, and uklonskovite (Sabelli, 1984, 1985a, b; Sabelli and Brizzi, 1984; Sabelli and Santucci, 1987). Moreover, Sabelli and Santucci (1987) identified a potential new mineral species associated with jurbanite, alunogen, and gypsum. This species was described as a basic aluminum sulfate with the chemical formula $Al_3(SO_4)_2(OH)_5 \cdot 9H_2O$ and triclinic symmetry. However, the poor quality of the available crystals did not allow a full characterization of this species that remained unnamed. It was indeed reported as UM1987-12-SO:AlH by Smith and Nickel (2007).

The examination of a suite of mineral specimens from several Italian localities performed in collaboration with the Associazione Micro-mineralogica Italiana led to the identification of an interesting sample collected at the Cetine di Cotorniano Mine by the amateur mineralogist Massimo Batoni. The specimen is characterized by a few rounded aggregates, up to 1 mm in diameter, formed by white tabular crystals. X-ray diffraction and chemical analyses showed that this sample corresponded to UM1987-12-SO : AlH, and the single-crystal X-ray diffraction study allowed the solution of the crystal structure of this mineral, confirming its novelty.

The mineral and its name, batoniite, were approved by the Commission on New Minerals, Nomenclature and Classification of the International Mineralogical Association (CNMNC-IMA) under voting number 2023-008. The name honors Massimo Batoni (born 6 April 1948) for his contribution to the knowledge of Italian mineralogy. He provided the first specimens of manganiceladonite (Lepore et al., 2017) and batoniite. Moreover, he is the co-author of a book about the history and mineralogy of the Cetine di Cotorniano Mine (Menchetti and Batoni, 2015), and he is currently the vice president of the Associazione Micro-mineralogica Italiana. The holotype material is deposited in the mineralogical collection of the Museo di Storia Naturale, University of Pisa, Via Roma 79, Calci (Pisa), under catalogue number 20028.

This paper describes the new mineral species batoniite and discusses its crystal chemistry.

2 Occurrence and physical properties

Batoniite was identified in a sample collected at the Cetine di Cotorniano Mine (43°13′ N, 11°09′ E), Chiusdino, province of Siena, Tuscany. This mine exploited, between 1878 and 1948, an Sb ore deposit (Menchetti and Batoni, 2015, and references therein) whose origin is related to the widespread hydrothermal activity that has been developing in southern Tuscany since the Late Miocene and is associated with the Neogene–Quaternary magmatism of the Tuscan Magmatic Province (e.g., Lattanzi, 1999; Dini, 2003; Sillitoe and Brogi, 2021). The mineralization consists of jasperoid and vuggy silica masses replacing host rocks ("Calcare Cavernoso" Formation of Upper Triassic age) at the contact with the overlying argillic formations belonging to the Liguride Nappe. Ore minerals are mainly represented by stibnite, whereas iron sulfides (pyrite, marcasite) are accessory phases. Before the approval of batoniite, the Cetine di Cotorniano Mine was the type locality for four other mineral species, i.e., brizziite, cetineite, onoratoite, and rosenbergite (Belluomini et al., 1968; Sabelli and Vezzalini, 1987; Olmi et al., 1993; Olmi and Sabelli, 1994). Moreover, in addition to the sulfate assemblages cited in the Introduction, the Cetine di Cotorniano Mine is also known for the occurrence of some rare halides (elpasolite, hydrokenoralstonite, in addition to the new species onoratoite and rosenbergite – Menchetti and Batoni, 2015).

In type material, batoniite occurs as hemispherical aggregates, up to 1 mm in diameter, formed by tabular crystals, flattened on {011} (Fig. 1). Batoniite is colorless to white, with a white streak and a vitreous to greasy luster. The mineral is not fluorescent under either shortwave or longwave ultraviolet light. Mohs hardness was not determined, owing to the paucity of available material and its brittleness. Indeed, batoniite shows a {011} perfect cleavage; there are other less distinct cleavage surfaces, but their crystallographic orientation was not determined. The calculated density, based on the ideal formula and single-crystal X-ray diffraction unit-cell parameters, is 1.949 g cm^{-3}. Batoniite is slowly soluble in H_2O.

Batoniite is colorless and non-pleochroic under plane-polarized light, with a distinct cleavage and inclined extinction (extinction angle $\sim 30°$). It is biaxial negative with $\alpha = 1.4833(6)$, $\beta = 1.4948(6)$, and $\gamma = 1.5019(5)$, measured at 589 nm light. The angle $2V$ determined by spindle stage is 71(1)°, to be compared with that calculated by the equation of Wright (1951) = 75.8°. X is inclined $\sim 60°$ to (011). The Gladstone–Dale relationship (Mandarino, 1979, 1981) is 0.0022 (superior).

In type material, batoniite is associated with gypsum and a poorly crystalline resinous orange-brownish, still undetermined Al–Fe sulfate. The specimen was collected in the Garibaldi Tunnel, the lowest mining level of the Cetine di Cotorniano Mine; these mining works were excavated within Paleozoic metasediments underlying the Calcare Cavernoso Formation.

3 Experiment

3.1 Raman spectroscopy

Micro-Raman spectra were collected on a sample of batoniite in the range 4000–100 cm^{-1} using a DXR dispersive Raman spectrometer (Thermo Scientific) mounted on a confocal Olympus microscope (Department of Mineralogy and Petrology, National Museum, Czech Republic). The Raman signal was excited by an unpolarized, green, 532 nm, solid-

Figure 1. Batoniite, aggregate of white tabular crystals with colorless prismatic crystals of gypsum and orange-brown resinous unidentified Al–Fe sulfate. Garibaldi Tunnel, Cetine di Cotorniano Mine, Chiusdino, Siena, Tuscany, Italy. Type material. Catalogue number 20028, Museo di Storia Naturale, Università di Pisa. Photo: Daniela Mauro.

state, diode-pumped laser and detected by a CCD detector. The experimental parameters were a 100× objective, a 10 s exposure time, 100 exposures, a 50 µm pinhole spectrograph aperture, and a 6 mW laser power level. The possible thermal damage of the measured points was excluded by visual inspection of excited surface after measurement, by checking for the decay of the spectral lines at the start of excitation and for thermal downshift of Raman lines. The instrument was set up by a software-controlled calibration procedure using multiple neon emission lines (wavelength calibration), multiple polystyrene Raman bands (laser frequency calibration), and standardized white-light sources (intensity calibration). Spectral manipulations were performed using the OMNIC 9 software (Thermo Scientific).

3.2 Chemical data

Quantitative chemical analyses were carried out using a CAMECA SX 100 electron microprobe (WDS mode, 15 kV, 8 nA, 5 µm beam diameter) on an unpolished crystal surface at the National Museum, Prague, Czech Republic. Any attempt to prepare a polished surface was unsuccessful, owing to the brittleness of batoniite and its slow solubility in H_2O. Standards (element, emission line) were sanidine (Al$K\alpha$), hematite (Fe$K\alpha$), and celestine (S$K\alpha$). Contents of other elements with atomic numbers > 8 are below detection limits. Matrix correction by PAP software (Pouchou and Pichoir, 1985) was applied to the data. Results of chemical analyses (average of 12 spot analyses) are given in Table 1.

Table 1. Chemical data (in wt %) for batoniite. n – number of spot analyses.

Constituent	Mean	Range ($n = 12$)	SD	Normalized
Al_2O_3	33.48	31.60–36.28	1.17	30.17
Fe_2O_3	0.05	0–0.18	0.07	0.05
SO_3	33.00	30.86–36.97	1.55	29.74
Sum	66.53	62.46–73.25	2.64	
$H_2O^*_{calc}$	44.41			40.04
Total	110.94			100.00

* Calculated according to stoichiometry.

3.3 X-ray crystallography

Intensity data were collected using a Bruker D8 Venture diffractometer equipped with an air-cooled Photon III CCD detector and microfocus Mo$K\alpha$ radiation (C.I.S.U.P., University of Pisa, Italy). The detector-to-crystal distance was 38 mm. Data were collected using ω and φ scan modes, in 0.5° slices, with an exposure time of 5 s per frame. A total of 2424 frames were collected. The frames were integrated with the Bruker SAINT software package using a narrow-frame algorithm. Data were corrected for Lorentz polarization, absorption, and background using the package of software *Apex*4 (Bruker AXS, 2022). Unit-cell parameters were refined on the basis of the XYZ centroid of 9840 reflections above $20\sigma(I)$ with $4.79° < 2\theta < 54.90°$. They are $a = 9.1757(6)$, $b = 12.0886(9)$, $c = 20.9218(15)$ Å, $\alpha = 82.901(3)$, $\beta = 87.334(3)$, $\gamma = 86.999(2)°$, $V = 2297.8(3)$ Å^3, and $Z = 2$. The $a : b : c$ ratio is 0.7590 : 1 : 1.7307.

The statistical tests on the distribution of $|E|$ values ($|E^2 - 1| = 0.891$) suggest the possible occurrence of a center of symmetry. The crystal structure of batoniite was solved through direct methods using *Shelxtl* (Sheldrick, 2015) in the space group $P\overline{1}$ and refined through *Shelxl*-2018 (Sheldrick, 2015). Neutral scattering curves, taken from the *International Tables for Crystallography* (Wilson, 1992), were used. Eight independent Al sites and five S sites were located. Reiterate difference-Fourier maps allowed 57 O and 60 H atoms to be located. Restraints on the O–H distances were applied, and the isotropic displacement parameter of H atoms was constrained to be 1.5 times that of the O atoms to which they are bonded. After several cycles of anisotropic refine-

Table 2. Summary of parameters describing data collection and refinement for batoniite.

Crystal data	
Crystal size (mm)	$0.150 \times 0.138 \times 0.040$
Cell setting, space group	Triclinic, $P\bar{1}$
a (Å)	9.1757(6)
b (Å)	12.0886(9)
c (Å)	20.9218(15)
α (°)	82.901(3)
β (°)	87.334(3)
γ (°)	86.999(2)
V(Å^3)	2297.8(3)
Z	2
Data collection and refinement	
Radiation, wavelength (Å)	Mo$K\alpha$, 0.71073
Temperature (K)	293(2)
$2\theta_{max}$ (°)	55.10
Measured reflections	65912
Unique reflections	10076
Reflections with $F_o > 4\sigma(F_o)$	8118
R_{int}	0.0822
$R\sigma$	0.0566
Range of h, k, l	$-11 \le h \le 11$, $-15 \le k \le 15$, $-26 \le l \le 25$
R [$F_o > 4\sigma(F_o)$]	0.0916
R (all data)	0.1096
wR (on F_o^2)*	0.1837
Goodness of fit	1.233
Number of least-squares parameters	811
Maximum and minimum	1.03 [at 1.47 Å from O(43)]
Residual peak (e^- Å^{-3})	−0.69 [at 0.87 Å from H(19)]

* $w = 1/[\sigma^2(F_o^2) + (0.0001P)^2 + 25.4979P]$.

ment (but for H atoms, refined isotropically), the R_1 factor converged to 0.0916 for 8118 unique reflections with $F_o > 4\sigma(F_o)$ and 811 refined parameters. Details of the data collection and crystal structure refinement are given in Table 2. Atom coordinates and isotropic or equivalent isotropic displacement parameters are reported in the crystallographic information file, available in the Supplement. Tables 3 and 4 give selected bond distances and H-bonds, respectively. Bond-valence calculation, shown in Table S1, was performed using the bond parameters of Brese and O'Keeffe (1991).

Owing to the very small amount of pure material and its small size, X-ray powder diffraction data were collected using a Bruker D8 Venture single-crystal diffractometer equipped with a Photon III CCD area detector (microfocus Cu$K\alpha$ radiation) simulating a Gandolfi-like geometry. Observed X-ray diffraction lines are reported in Table S2, along with the calculated pattern based on the structural model discussed below.

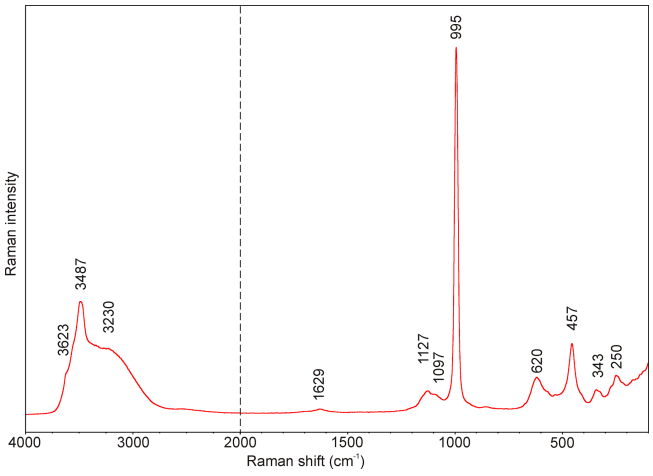

Figure 2. Raman spectrum of batoniite in the range 4000–100 cm^{-1}, split at 2000 cm^{-1}.

4 Results and discussion

4.1 Raman spectrum of batoniite

The Raman spectrum of batoniite is given in Fig. 2. The main bands in the region between 1200 and 100 cm^{-1} are 1127, 1097, 995, 620, 457, 343, and 250 cm^{-1}. Its interpretation is based on the papers by Myneni (2000), Nakamoto (2009), and Čejka et al. (2011). The very strong Raman band at 995 cm^{-1} is attributed to ν_1 symmetric stretching vibration of SO_4 groups; the weak band at 1127 cm^{-1} with a shoulder at 1097 cm^{-1} is related to the triply degenerate ν_3 SO_4 antisymmetric stretching vibrations. The bands at 620 and 457 cm^{-1} may be attributed to the ν_4 and ν_2 bending vibrations of SO_4 groups. Finally, bands at 343 and 250 cm^{-1} are probably related to Al–φ (φ = OH, H_2O) and lattice modes. Presence of H_2O groups and hydroxyl ions is well-documented by a broad (O–H)-stretching band running from 3750 to 2800 cm^{-1} with components near 3623, 3487, and 3230 cm^{-1} (Fig. 2). According to the empirical relation of Libowitzky (1999), O–H···O hydrogen bond lengths vary in the range from 2.60 to > 3.20 Å, which are comparable to values inferred from crystal structure data. The band at 1629 cm^{-1} relates to ν_2 (δ) bending vibrations of H_2O groups.

4.2 Chemical formula of batoniite

The collection of high-quality chemical data for batoniite was a very difficult task, not only for the difficult preparation of a polished surface and the low amount of pure material preventing a direct determination of the H_2O content but also for the partial dehydration affecting this mineral under the high vacuum used for electron microprobe analysis. For this reason, after the addition of calculated H_2O, based

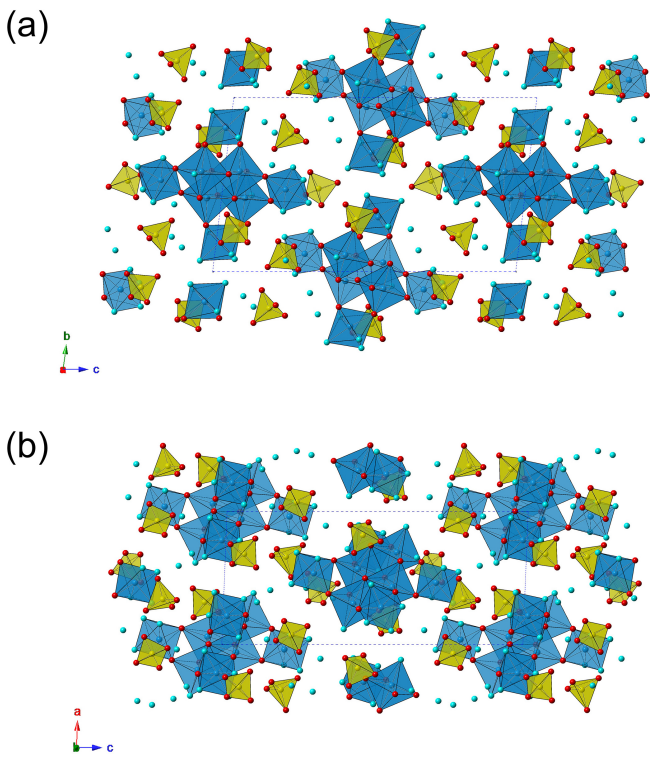

Figure 3. Crystal structure of batoniite, as seen down *a* **(a)** and *b* **(b)**. Symbols: blue polyhedra – Al-centered octahedra; yellow – S-centered tetrahedra. Circles: red – O and OH groups; light blue – H_2O groups. For the sake of clarity, H atoms are not shown.

on structural data, the total was very high, i.e., ca. 111 wt % (Table 1).

On the basis of Al + Fe + S = 13 atoms per formula unit, the empirical formula of batoniite is $(Al_{7.98}Fe_{0.01})_{\Sigma 7.99}(SO_4)_{5.01}(OH)_{13.95}(H_2O)_{18} \cdot 5H_2O$, where two different kinds of H_2O have been distinguished on the basis of structural information (see below). This formula agrees with the ideal one, $Al_8(SO_4)_5(OH)_{14}(H_2O)_{18} \cdot 5H_2O$, corresponding to (in wt %) SO_3 29.68, Al_2O_3 30.24, and H_2O 40.08, with a sum of 100.00.

4.3 Crystal structure of batoniite

The crystal structure of batoniite is formed by isolated $[Al_8(OH)_{14}(H_2O)_{18}]^{10+}$ polyoxometalate clusters, H-bond connected to five interstitial $(SO_4)^{2-}$ groups and five "free" H_2O groups (Fig. 3). In agreement with Hawthorne (1985) and Schindler and Hawthorne (2001), this structural arrangement can be described as a bipartite structure, with the polyoxometalate clusters representing the structural unit and (SO_4) and H_2O groups forming the interstitial complex.

Structural unit

The structural unit of batoniite is characterized by the polyoxocation $[Al_8(OH)_{14}(H_2O)_{18}]^{10+}$ (Fig. 4). Such a cluster was previously reported in some synthetic compounds, e.g., $[Al_8(OH)_{14}(H_2O)_{18}](SO_4)_5 \cdot 16H_2O$ (Casey et al., 2005). Two symmetry-independent $[Al_8(OH)_{14}(H_2O)_{18}]^{10+}$ polyoxocations occur in batoniite. Every cluster is formed by a core of edge-sharing Al octahedra, with two central $Al(OH)_6$ and two peripheral $Al(OH)_5(H_2O)$ polyhedra. In this tetrameric unit, Al–Al distances range between 2.923 and 2.947 Å, similar to those reported by Casey et al. (2005). The octamer is completed by four additional $Al(OH)_2(H_2O)_4$ octahedra connected to the core through corner sharing. Average < Al–O > distances vary between 1.892 and 1.903 Å, with single values between 1.845 and 1.981 Å. Bond-valence sums (BVSs) range between 3.04 and 3.15 valence units (vu), in agreement with the occurrence of Al^{3+}. According to electron microprobe analysis, a negligible replacement of Al by Fe^{3+} occurs. The $[Al_8(OH)_{14}(H_2O)_{18}]^{10+}$ cluster is a novel kind of polyoxocation among minerals. Recently, Kampf et al. (2020, 2022) identified two different Al-bearing polyoxocations in caseyite and protocaseyite. In the former, the vanadoaluminate heteropolycation $[(V^{5+}O_2)Al_{10}(OH)_{20}(H_2O)_{18}]^{11+}$ was identified; it is a derivate of the "flat-Al_{13}" polyoxocation $[Al_{13}(OH)_{24}(H_2O)_{24}]^{15+}$ reported at the end of the 1990s and so far never observed in minerals (Seichter et al., 1998; Casey, 2006). Protocaseyite shows a different kind of polycation, which is the linear tetrameric isopolycation $[Al_4(OH)_6(H_2O)_{12}]^{6+}$. Batoniite is a further addition to this group of species showing sheets of Al^{3+}-centered octahedra colloquially referred to as "flatimers" (Kampf et al., 2022).

Interstitial complex

The interstitial complex of batoniite is represented by five (SO_4) and five H_2O groups, H-bonded to the structural unit. Isolated (SO_4) groups have average bond distances ranging between 1.456 and 1.470 Å, slightly shorter than the grand value given by Hawthorne et al. (2000) for S–O bonds, i.e., 1.473 Å. This results in BVS values in the range 6.08–6.30 vu. Oxygen atoms of (SO_4) groups act as acceptors of H-bonds from both the structural unit and the five H_2O groups belonging to the interstitial complex (Table 4). Their BVSs vary between 1.71 and 2.18 vu, the minimum and maximum values being affected by the geometry of the H-bonds involving O(15) (see below).

"Free" H_2O groups are acceptors of H-bonds from the structural unit (and, limited to Ow(1), also from another "free" H_2O group at Ow(5)), and they act as donors to O atoms belonging to (SO_4) groups (Table 4). Their BVSs range between −0.07 and 0.15 vu.

Table 3. Selected bond distances (in Å) for batoniite.

Al(1)	–O(2)	1.854(5)	Al(2)	–O(10)	1.855(5)	Al(3)	–O(3)	1.850(5)	Al(4)	–O(12)	1.850(5)
	–O(3)	1.860(5)		–O(8)	1.875(5)		–O(10)	1.860(5)		–O(8)	1.853(5)
	–O(6)	1.889(5)		–O(9)	1.881(5)		–O(12)	1.865(5)		–O(14)	1.888(5)
	–O(5)	1.901(5)		–O(2)	1.888(5)		–O(9)	1.872(4)		–O(15)	1.911(5)
	–O(1)	1.915(5)		–O(11)	1.905(5)		–O(7)	1.968(5)		–O(13)	1.954(5)
	–O(4)	1.957(5)		–O(7)	1.946(4)		–O(7)	1.972(5)		–O(16)	1.964(5)
	average	1.896		average	1.892		average	1.898		average	1.903
Al(5)	–O(19)	1.845(5)	Al(6)	–O(23)	1.854(5)	Al(7)	–O(19)	1.868(5)	Al(8)	–O(23)	1.856(5)
	–O(18)	1.856(5)		–O(18)	1.861(4)		–O(27)	1.871(5)		–O(28)	1.860(5)
	–O(22)	1.910(5)		–O(24)	1.867(4)		–O(24)	1.880(4)		–O(29)	1.904(5)
	–O(21)	1.915(5)		–O(26)	1.872(5)		–O(28)	1.894(5)		–O(31)	1.906(5)
	–O(17)	1.931(5)		–O(25)	1.973(4)		–O(26)	1.922(5)		–O(30)	1.945(5)
	–O(20)	1.932(5)		–O(25)	1.981(5)		–O(25)	1.933(4)		–O(32)	1.946(5)
	average	1.898		average	1.901		average	1.895		average	1.903
S(1)	–O(34)	1.458(5)	S(2)	–O(40)	1.444(5)	S(3)	–O(42)	1.436(6)	S(4)	–O(46)	1.445(6)
	–O(35)	1.467(5)		–O(37)	1.465(5)		–O(43)	1.454(6)		–O(47)	1.456(5)
	–O(33)	1.475(5)		–O(39)	1.470(5)		–O(44)	1.457(6)		–O(48)	1.460(6)
	–O(36)	1.480(5)		–O(38)	1.487(5)		–O(41)	1.476(6)		–O(45)	1.477(5)
	average	1.470		average	1.467		average	1.456		average	1.460
S(5)	–O(52)	1.451(5)									
	–O(50)	1.462(5)									
	–O(51)	1.467(5)									
	–O(49)	1.469(5)									
	average	1.462									

Hydrogen bonding

Bond-valence calculations (Table S1) highlight that all the anion positions occurring in batoniite are underbonded. In particular, three groups of anions can be distinguished: the first group has a BVS ~ 1.5 vu, whereas the second and the third ones have BVSs of ~ 1.2–1.3 and ~ 0.5 vu, respectively.

The first group is represented by O atoms bonded to S atoms. As reported above, every O atom is an acceptor of H-bonds from (OH) groups and H_2O belonging to the aluminate polyoxocations and from "free" H_2O groups. Table 4 reports details of H-bonds in batoniite, whereas Table S1 gives the BVSs after the addition of the contribution of H-bonds calculated according to the relation of Ferraris and Ivaldi (1988). The only uncertainty seems to be represented by the configuration of H-bonds around O(38) and O(40). Both sites belong to the S(2)-centered tetrahedron. Indeed, two possible bonds involving the H atom at the H(152) site could occur, i.e., O(15)–H(152)···O(40) and O(15)–H(152)···O(38). The former gives rise to an O(35)···O(15)···O(40) angle of $\sim 80°$, whereas the latter would show an O(35)···O(15)···O(38) angle close to 100°. In agreement with Ferraris and Franchini-Angela (1972), the latter angular value is more reasonable for an H-bond involving H_2O groups. In Table S1 both possible configurations are reported, even if the most probable H-bond is that between O(15) and O(38). In this way, the overbonding at O(40) would be removed, and the undersaturation of O(38) would be reduced. If so, the BVS of O atoms belonging to (SO_4) groups would range between 1.83 and 2.16 vu.

The second and third group of underbonded anions is represented by (OH) and H_2O groups, respectively. The former belong to the polyoxocations only and are a donor of H-bonds to both the O atoms of (SO_4) groups and "free" H_2O groups. Usually, H···O distances are in the range 1.7–2.1 Å, but some very long distances were observed, i.e., H(9)···O(37) = 2.62(5) Å and H(24)···O(44) = 2.51(6) Å. These long distances result in long O···O distances, i.e., O(9)···O(37) = 3.471(7) Å and O(24)···O(44) = 3.225(8) Å. These distances are out of the range proposed by Ferraris and Franchini-Angela (1972) for H···O and O···O distances compatible with H-bonds (up to 2.2–2.3 and 3.1–3.2 Å, respectively). In Table S1, these are considered very weak H-bonds. After correction for H-bonds, the BVSs for (OH) groups range between 0.93 and 1.13 vu.

H_2O groups are bonded to the polyoxocation clusters or can occur in the interstitial complex. The former act as donors of H-bonds to O atoms of (SO_4) groups as well as to "free" H_2O groups, whereas the latter are both acceptors and donors of H-bonds. Also in this case, a long H···O contact was observed, i.e., H(w32)···O(47) = 2.57(11) Å, with a resulting O···O distance of 3.264(11) Å and a small Ow(3)–H(w32)···O(47) angle of 132(11)°. Moreover, among H_2O

Table 4. Details of hydrogen bonding in batoniite. Bond strengths were calculated according to Ferraris and Ivaldi (1988). D – donor; A – acceptor.

D–H···A	D–H (Å)	H···A (Å)	D···A (Å)	Angle D–H···A (°)	Bond strength (vu)
O(1)–H(011)···O(40)	0.89(5)	1.80(5)	2.662(8)	162(8)	0.25
O(1)–H(012)···O(34)	0.89(4)	1.87(5)	2.752(7)	172(8)	0.20
O(2)–H(2)···O(36)	0.85(4)	2.00(5)	2.841(6)	168(7)	0.17
O(3)–H(3)···Ow(4)	0.89(4)	2.08(5)	2.912(7)	155(7)	0.15
O(4)–H(41)···O(43)	0.90(5)	1.87(5)	2.767(8)	173(8)	0.20
O(4)–H(42)···O(51)	0.89(4)	1.78(5)	2.669(6)	173(8)	0.24
O(5)–H(51)···O(48)	0.92(4)	1.73(5)	2.646(7)	173(8)	0.26
O(5)–H(52)···O(50)	0.92(4)	1.71(5)	2.628(7)	171(8)	0.27
O(6)–H(61)···O(47)	0.94(4)	1.66(5)	2.591(7)	171(8)	0.29
O(6)–H(62)···O(49)	0.94(4)	1.75(5)	2.672(6)	168(8)	0.24
O(7)–H(7)···O(40)	0.87(4)	2.01(5)	2.869(7)	174(7)	0.16
O(8)–H(8)···O(36)	0.92(4)	1.92(5)	2.839(7)	171(7)	0.17
O(9)–H(9)···O(37)	0.89(4)	2.62(5)	3.471(7)	161(7)	0.08
O(10)–H(10)···Ow(3)	0.89(4)	1.96(5)	2.790(8)	154(7)	0.19
O(11)–H(111)···O(37)	0.87(4)	1.85(5)	2.707(7)	168(8)	0.22
O(11)–H(112)···O(49)	0.89(5)	1.92(5)	2.773(8)	159(8)	0.19
O(12)–H(12)···Ow(3)	0.89(4)	2.03(5)	2.869(9)	157(8)	0.16
O(13)–H(131)···O(39)	0.91(4)	2.03(5)	2.938(8)	173(8)	0.14
O(13)–H(132)···O(35)	0.92(5)	1.83(5)	2.744(7)	177(9)	0.21
O(14)–H(141)···Ow(4)	0.91(5)	1.73(5)	2.639(8)	180(9)	0.26
O(14)–H(142)···O(37)	0.94(4)	1.82(5)	2.757(8)	174(8)	0.20
O(15)–H(151)···O(35)	0.91(5)	1.75(5)	2.647(7)	170(8)	0.26
O(15)–H(152)···O(40)	0.90(4)	2.12(6)	2.935(8)	150(8)	0.14
O(15)–H(152)···O(38)	0.90(4)	2.29(6)	3.063(8)	144(7)	0.12
O(16)–H(161)···O(39)	0.90(5)	2.15(5)	3.014(8)	160(8)	0.13
O(16)–H(162)···O(38)	0.94(4)	1.71(5)	2.648(7)	174(8)	0.26
O(17)–H(171)···Ow(1)	0.94(5)	1.69(5)	2.631(8)	173(9)	0.27
O(17)–H(172)···O(43)	0.90(4)	1.83(5)	2.710(7)	167(9)	0.22
O(18)–H(18)···Ow(5)	0.91(4)	1.95(5)	2.852(7)	169(7)	0.17
O(19)–H(19)···O(51)	0.91(4)	1.98(5)	2.833(7)	154(7)	0.17
O(20)–H(201)···O(48)	0.93(5)	1.70(5)	2.634(8)	178(8)	0.26
O(20)–H(202)···O(41)	0.92(5)	1.90(5)	2.774(8)	159(8)	0.19
O(21)–H(211)···O(44)	0.92(4)	1.88(5)	2.755(8)	159(8)	0.20
O(21)–H(212)···O(45)	0.92(5)	1.77(5)	2.688(7)	178(8)	0.23
O(22)–H(221)···O(52)	0.93(5)	1.71(5)	2.621(8)	165(8)	0.27
O(22)–H(222)···O(41)	0.87(4)	2.07(5)	2.939(8)	174(8)	0.14
O(23)–H(23)···O(45)	0.90(4)	1.83(5)	2.730(6)	175(8)	0.21
O(24)–H(24)···O(44)	0.90(4)	2.51(6)	3.225(8)	136(6)	0.10
O(25)–H(25)···O(42)	0.90(4)	1.85(5)	2.741(7)	170(7)	0.21
O(26)–H(26)···O(44)	0.89(4)	2.34(5)	3.185(7)	159(7)	0.10
O(27)–H(271)···Ow(2)	0.93(4)	1.60(5)	2.525(8)	171(9)	0.35
O(27)–H(272)···O(44)	0.93(5)	1.92(5)	2.844(9)	174(8)	0.17
O(28)–H(28)···O(51)	0.90(4)	2.00(5)	2.892(7)	169(7)	0.15
O(29)–H(291)···Ow(5)	0.93(4)	1.76(5)	2.687(8)	176(8)	0.23
O(29)–H(292)···O(33)	0.92(4)	1.81(5)	2.723(6)	171(8)	0.22
O(30)–H(301)···O(39)	0.90(5)	1.93(5)	2.825(8)	168(8)	0.17
O(30)–H(302)···O(36)	0.93(4)	1.77(5)	2.694(6)	174(8)	0.23
O(31)–H(311)···O(42)	0.91(5)	1.74(5)	2.647(8)	170(8)	0.26
O(31)–H(312)···O(50)	0.92(4)	1.75(5)	2.665(7)	175(8)	0.25
O(32)–H(321)···O(34)	0.91(4)	1.83(5)	2.732(7)	168(8)	0.21
O(32)–H(322)···O(46)	0.92(4)	1.78(5)	2.681(7)	166(8)	0.24
Ow(1)–H(w11)···O(47)	0.93(5)	2.03(5)	2.958(10)	173(10)	0.14
Ow(1)–H(w12)···O(41)	0.92(5)	2.08(8)	2.843(10)	139(9)	0.17
Ow(2)–H(w21)···O(33)	0.97(5)	1.84(6)	2.781(9)	162(9)	0.19
Ow(2)–H(w22)···O(45)	0.98(5)	1.73(5)	2.702(7)	174(9)	0.23
Ow(3)–H(w31)···O(33)	0.93(5)	2.31(10)	3.002(9)	131(10)	0.13
Ow(3)–H(w32)···O(47)	0.93(5)	2.57(11)	3.264(11)	132(11)	0.10
Ow(4)–H(w41)···O(46)	0.92(5)	1.91(6)	2.747(8)	150(9)	0.20
Ow(4)–H(w42)···O(49)	0.93(5)	2.00(5)	2.921(7)	172(8)	0.15
Ow(5)–H(w51)···Ow(1)	0.92(5)	1.86(5)	2.772(9)	175(10)	0.19
Ow(5)–H(w52)···O(52)	0.90(5)	2.28(8)	2.934(7)	129(8)	0.14

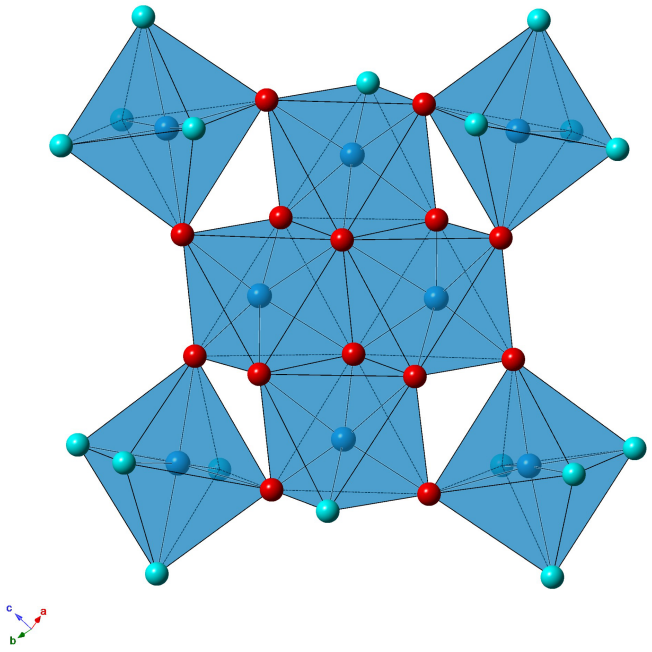

Figure 4. The $[Al_8(OH)_{14}(H_2O)_{18}]^{10+}$ octamer. Same symbols as in Fig. 3. For the sake of clarity, H atoms are not shown.

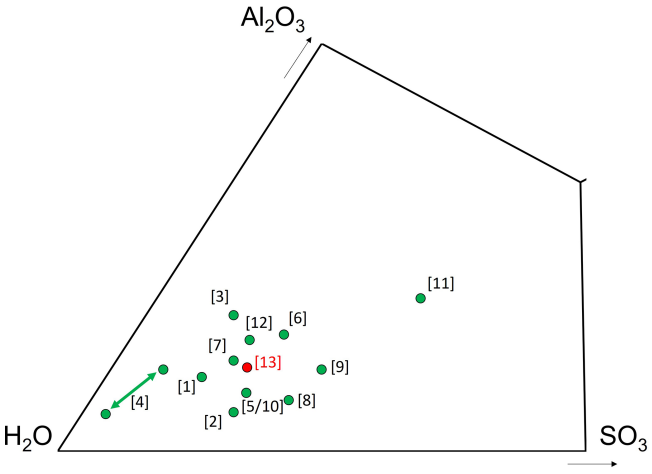

Figure 5. Chemical composition of batoniite, expressed as mol % in the ternary system Al_2O_3–H_2O–SO_3. [1] Aluminite, $Al_2(SO_4)(OH)_4 \cdot 7H_2O$; [2] alunogen, $Al_2(SO_4)_3 \cdot 17H_2O$; [3] felsőbányaite, $Al_4(SO_4)(OH)_{10} \cdot 4H_2O$; [4] hydrobasaluminite, $Al_4(SO_4)(OH)_{10} \cdot 12–36H_2O$ (in the IMA list the number of H_2O groups is given as 15); [5] jurbanite, $Al(SO_4)(OH) \cdot 5H_2O$; [6] mangazeite, $Al_2(SO_4)(OH)_4 \cdot 3H_2O$; [7] meta-aluminite, $Al_2(SO_4)(OH)_4 \cdot 5H_2O$; [8] meta-alunogen, $Al_2(SO_4)_3 \cdot 12H_2O$; [9] riotintoite, $Al(SO_4)(OH) \cdot 3H_2O$; [10] rostite, $Al(SO_4)(OH) \cdot 5H_2O$; [11] schlossmacherite, $(H_3O)Al_3(SO_4)_2(OH)_6$; [12] zaherite, $Al_{12}(SO_4)_5(OH)_{26} \cdot 20H_2O$; [13] batoniite, $Al_8(SO_4)_5(OH)_{14} \cdot 23H_2O$.

groups, one is involved in a very strong H-bond, i.e., O(27)–H(271)···Ow(2), showing short H···O and O···O distances of 1.60(5) and 2.525(8) Å. It is worth noting that Ferraris and Franchini-Angela (1972) never found H···O and O···O distances shorter than 1.65 and 2.60 Å, respectively. After the correction for H-bonds, the BVSs of H_2O groups range between −0.07 and 0.15 vu.

The discrepancies outlined above with the values reported by Ferraris and Franchini-Angela (1972) are probably related to the relatively low quality of the structure refinement. Indeed, the estimated standard deviations associated with the observed bond distances and angles involving H atoms are quite large. However, notwithstanding these minor shortcomings, the crystal structure of batoniite shows a well-ordered atomic arrangement. Its crystal-chemical formula, considering its bipartite nature, can be correctly written as $[Al_8(OH)_{14}(H_2O)_{18}](SO_4)_5 \cdot 5H_2O$ ($Z = 2$).

4.4 Genesis of batoniite

Aluminum sulfates are common secondary minerals usually related to the action of SO_4-rich solutions on Al-bearing rocks. This condition can be observed in different geological settings, e.g., in acid mine drainage systems (e.g., Bigham and Nordstrom, 2000) as well as in fumarolic and hydrothermal environments (e.g., Martin et al., 1999; Zimbelman et al., 2005).

The crystallization of batoniite is probably related to the action of H_2SO_4, produced through the oxidation of pyrite, on Al-bearing rocks in the Garibaldi Tunnel, where Paleozoic metasediments crop out. In the same occurrence, other Al-bearing sulfates are known, such as jurbanite and alunogen (e.g., Sabelli and Santucci, 1987). The genesis of batoniite agrees with the hypothesis of Perkins et al. (2017), who proposed that (Al-octamer)-bearing phases could form in natural environments by dissolution of Al-bearing minerals in acidic sulfate solutions, such as those occurring in acid mine drainage systems.

4.5 Hydrated aluminum sulfates: a short review and comparison with batoniite

Thirteen hydrous aluminum sulfate species are known (Table 5), and in the ternary system Al_2O_3–H_2O–SO_3 they are restricted to a relatively small area close to the H_2O corner (Fig. 5), in keeping with the study of Basset and Goodwin (1949). In addition, the anhydrous aluminum sulfate millosevichite, $Al_2(SO_4)_3$ (Panichi, 1913), can be considered.

The crystal structures of these species display different kinds of Al-bonding environments. Indeed, this element, always occurring in octahedral coordination, can be bonded to O^{2-}, $(OH)^-$, and H_2O groups, forming isolated polyhedra or clusters showing different sizes.

Alunogen and its dehydration product meta-alunogen are characterized by isolated $Al(H_2O)_6$ octahedra, connected through H-bonds to isolated (SO_4) groups and free H_2O

Table 5. Currently valid mineral species belonging to the Al_2O_3–H_2O–SO_3 ternary system.

Mineral	Chemical formula*	a (Å)	b (Å)	c (Å)	α (°)	β (°)	γ (°)	Space group
Aluminite[1]	$Al_2(SO_4)(OH)_4(H_2O)_3 \cdot 4H_2O$	7.44	15.58	11.70	90	110.2	90	$P2_1/c$
Alunogen[2]	$Al_2(SO_4)_3(H_2O)_{12} \cdot 5H_2O$	7.42	26.97	6.06	89.9	97.6	91.9	$P\bar{1}$
Batoniite[3]	$Al_8(SO_4)_5(OH)_{14}(H_2O)_{18} \cdot 5H_2O$	9.18	12.09	20.92	82.9	87.3	87.0	$P\bar{1}$
Felsőbányaite[4]	$Al_4(SO_4)(OH)_{10}(H_2O) \cdot 3H_2O$	13.03	10.02	11.12	90	104.3	90	$P2_1$
Hydrobasaluminite[5]	$Al_4(SO_4)(OH)_{10} \cdot 15H_2O$	14.91	9.99	13.64	90	112.4	90	n.d.
Jurbanite[6]	$Al(SO_4)(OH)(H_2O)_4 \cdot H_2O$	8.40	12.48	8.15	90	101.9	90	$P2_1/n$
Mangazeite[7]	$Al_2(SO_4)(OH)_4 \cdot 3H_2O$	8.29	9.38	11.35	96.1	98.9	96.6	n.d.
Meta-aluminite[8]	$Al_2(SO_4)(OH)_4(H_2O)_3 \cdot 2H_2O$	7.93	16.88	7.35	90	106.7	90	n.d.
Meta-alunogen[9]	$Al_2(SO_4)_3(H_2O)_{12} \cdot 2H_2O$	14.35	12.49	6.09	92.7	96.7	100.8	$P\bar{1}$
Riotintoite[10]	$Al(SO_4)(OH)(H_2O)_3$	5.60	7.45	7.67	74.8	86.0	75.8	$P\bar{1}$
Rostite[11]	$Al(SO_4)(OH)(H_2O)_5$	11.17	13.04	10.87	90	90	90	$Pcab$
Schlossmacherite[12]	$(H_3O)Al_3(SO_4)_2(OH)_6$	7.00	7.00	16.67	90	90	120	$R\bar{3}m$
Zaherite[13,14]	$Al_{12}(SO_4)_5(OH)_{26} \cdot 20H_2O$	18.48	19.45	3.77	95.2	91.5	80.2	n.d.

[1] Sabelli and Trosti Ferroni (1978). [2] Fang and Robinson (1976). [3] This work. [4] Farkas and Pertlik (1997). [5] Clayton (1980). [6] Sabelli (1985a). [7] Gamyanin et al. (2006). [8] Farkas and Werner (1980). [9] Kahlenberg et al. (2017). [10] Chukanov et al. (2016). [11] Čech (1979). [12] Schmetzer et al. (1980). [13] Beukes et al. (1984). [14] de Bruyin et al. (1985). * When structural data are available, H_2O groups are distinguished between cation-bonded (within brackets) and "free" H_2O groups. n.d.: not determined.

groups (five in alunogen and only two in meta-alunogen) (Menchetti and Sabelli, 1974; Fang and Robinson, 1976; Kahlenberg et al., 2017). Isolated Al-centered octahedra also probably occur in rostite. Indeed, this phase should be the (OH)-analogue of khademite (Mauro et al., 2020, and references therein), and, in this respect, two different kinds of Al-centered octahedra should occur, i.e., $Al(H_2O)_6$ and $Al(OH)_2(H_2O)_4$. However, the actual status of rostite is questionable. In millosevichite, AlO_6 octahedra share corners with (SO_4) groups, forming a three-dimensional network (Dahmen and Gruehn, 1993).

In jurbanite, $Al(OH)_2(H_2O)_4$ octahedra form dimers, H-bonded to (SO_4) groups and a free H_2O group (Sabelli, 1985a); riotintoite shows a similar Al-dimer, but in this case (SO_4) groups are corner-shared with Al-centered octahedra forming electroneutral $[Al_2(SO_4)_2(OH)_2(H_2O)_6]$ clusters (Chukanov et al., 2016).

Batoniite shows the peculiar $[Al_8(OH)_{14}(H_2O)_{18}]^{10+}$ octamer, hitherto known only in synthetic compounds (e.g., Casey et al., 2005; Perkins et al., 2017). As described above, H-bonds connect this polyoxocation to (SO_4) groups and "free" H_2O groups. In aluminite, Sabelli and Trosti Ferroni (1978) pointed out the presence of $[Al_4(OH)_8(H_2O)_6]^{4+}$ clusters formed by four edge-sharing Al octahedra. These clusters are then polymerized to form chains, running along the a axis and connected to isolated (SO_4) groups through H-bonds. Two different Al-centered octahedra, i.e., $Al(OH)_5(H_2O)$ and $Al(OH)_4(H_2O)_2$, occur in aluminite.

Finally, sheets of Al-centered octahedra are known in schlossmacherite and felsőbányaite. The former belongs to the alunite supergroup (Bayliss et al., 2010). These compounds are characterized by layers of corner-sharing $B(OH)_4O_2$ octahedra; in schlossmacherite, $B = Al^{3+}$. Felsőbányaite has $[Al_8(OH)_{20}(H_2O)_2]^{4+}$ layers, H-bonded to free H_2O groups, and (SO_4) tetrahedra. Two kinds of Al-centered octahedra occur, i.e., $Al(OH)_6$ and $Al(OH)_5(H_2O)$ (Farkas and Pertlik, 1997).

Currently, the crystal structure of some Al minerals (hydrobasaluminite, mangazeite, meta-aluminite, and zaherite) remains unknown. Hydrobasaluminite and meta-aluminite show relations with felsőbányaite and aluminite, respectively. Moreover, as shown in Fig. 5, meta-aluminite is chemically similar to batoniite; however, their X-ray powder diffraction patterns are distinctly different (Frondel, 1968). Mangazeite is another species considered similar to meta-aluminite, but in this case the X-ray powder diffraction pattern is different as well as its H_2O content, which is lower. Finally, zaherite has a distinctly higher Al / S atomic ratio; unfortunately, its crystal structure still remains to be solved.

5 Conclusions

Batoniite is a novel hydrated aluminum sulfate showing for the first time the natural occurrence of the $[Al_8(OH)_{14}(H_2O)_{18}]^{10+}$ polyoxocation, previously known in synthetic compounds (e.g., Casey et al., 2005). Thus, this species is a new addition to the small number of polyoxometalates (POMs) that currently constitute less than 1 % of all recognized minerals (Krivovichev, 2020). Usually, this kind of compound crystallized in low-temperature environments, in agreement with those hypothesized for batoniite. The description of this species adds further complexity to the crystal chemistry of aluminum sulfates, whose crystallization is related to different physical–chemical conditions (e.g., temperature, pH, relative humidity – Chou et al., 2013) and whose importance is due to their environmental and planetary significance.

As pointed out by Krivovichev (2020), the majority of minerals characterized by POM clusters have been discovered since the beginning of the 21st century, possibly as a result of the progress in experimental crystallography. Indeed, batoniite has been known since the end of the 1980s (Sabelli and Santucci, 1987), but its description has been possible only recently, due to the finding of suitable crystals and the possibility of collecting structural data on very small grains.

Finally, following the identification of batoniite and the previous contributions to the sulfate mineralogy given mainly by Sabelli and his co-workers during the 1980s (e.g., Sabelli and Brizzi, 1984; Sabelli and Santucci, 1987), the Cetine di Cotorniano Mine can be considered an interesting locality for the study of the mineralogy of secondary Al sulfates. Indeed, among the currently known 13 hydrated Al sulfates, 5 have been identified there, along with millosevichite and other mixed Al sulfates such as aluminocopiapite, alum-(K), alunite, halotrichite, pickeringite, tamarugite, and tschermigite (Menchetti and Batoni, 2015).

Data availability. The crystallographic information file data of batoniite are available in the Supplement.

Supplement. The supplement related to this article is available online at: https://doi.org/10.5194/ejm-35-703-2023-supplement.

Author contributions. CB and DM collected preliminary data. CB and DM carried out single-crystal X-ray diffraction. JS collected the micro-Raman spectrum, and JS and ZD performed electron microprobe analysis. RŠ collected optical data. DM wrote the paper, with input from the other authors.

Competing interests. At least one of the (co-)authors is a member of the editorial board of *European Journal of Mineralogy*. The peer-review process was guided by an independent editor, and the authors also have no other competing interests to declare.

Disclaimer. Publisher's note: Copernicus Publications remains neutral with regard to jurisdictional claims in published maps and institutional affiliations.

Special issue statement. This article is part of the special issue "New minerals: EJM support". It is not associated with a conference.

Acknowledgements. Massimo Batoni is acknowledged for providing us with the specimen of batoniite used for the mineralogical investigation. The comments of Sergey V. Krivovichev, Anthony R. Kampf, and an anonymous reviewer helped us to improve the paper.

Financial support. This research has been supported by the Ministry of Culture of the Czech Republic (long-term project DKRVO 2019–2023/1.II.e; National Museum, 00023272) for Jiří Sejkora and Zdeněk Dolníček.

Review statement. This paper was edited by Sergey Krivovichev and reviewed by Anthony Kampf and one anonymous referee.

References

Basset, H. and Goodwin, T. H.: The basic aluminum sulphates, J. Chem. Soc., 1949, 2239–2279, 1949.

Bayliss, P., Kolitsch, U., Nickel, E. H., and Pring, A.: Alunite supergroup: recommended nomenclature, Mineral. Mag., 74, 919–927, 2010.

Belluomini, G., Fornaseri, M., and Nicoletti, M.: Onoratoite, a new antimony oxychloride from Cetine di Cotorniano, Rosia (Siena, Italy), Mineral. Mag., 36, 1037–1044, 1968.

Beukes, G. J., Schoch, A. E., de Bruiyn, H., van der Westhuizen, W. A., and Bok, L. D. C.: A new occurrence of the hydrated aluminium sulphate zaherite, from Pofadder, South Africa, Mineral. Mag., 48, 131–135, 1984.

Biagioni, C., Pasero, M., and Zaccarini, F.: Tiberiobardiite, $Cu_9Al(SiO_3OH)(OH)_{12}(H_2O)_6(SO_4)_{1.5} \cdot 10H_2O$, a new mineral related to chalcophyllite from the Cretaio Cu prospect, Massa Marittima, Grosseto (Tuscany, Italy): Occurrence and crystal structure, Minerals, 8, 152, https://doi.org/10.3390/min8040152, 2018.

Biagioni, C., Bindi, L., and Kampf, A. R.: Crystal-chemistry of sulfates from the Apuan Alps (Tuscany, Italy), VII. Magnanelliite, $KFe_2^{3+}(SO_4)_4(OH)(H_2O)_2$, a new sulfate from the Monte Arsiccio mine, Minerals, 9, 779, https://doi.org/10.3390/min9120779, 2019a.

Biagioni, C., Bindi, L., Mauro, D., and Hålenius, U.: Crystal chemistry of sulfates from the Apuan Alps (Tuscany, Italy), V. Scordariite, $K_8(Fe^{3+}_{0.67}\square_{0.33})[Fe^{3+}_3O(SO_4)_6(H_2O)_3]_2(H_2O)_{11}$: a new metavoltine-related mineral, Minerals, 9, 702, https://doi.org/10.3390/min9110702, 2019b.

Biagioni, C., Bindi, L., Mauro, D., and Pasero, M.: Crystal-chemistry of sulfates from the Apuan Alps (Tuscany, Italy), IV. Giacovazzoite, $K_5Fe^{3+}_3O(SO_4)_6(H_2O)_9 \cdot H_2O$, the natural analogue of the β-Maus's Salt and its dehydration product, Phys. Chem. Miner., 47, 7, https://doi.org/10.1007/s00269-019-01076-4, 2020a.

Biagioni, C., Mauro, D., and Pasero, M.: Sulfates from the pyrite ore deposits of the Apuan Alps (Tuscany, Italy): A review, Minerals, 10, 1092, https://doi.org/10.3390/min10121092, 2020b.

Bigham, J. and Nordstrom, D. K.: Iron and aluminum hydroxysulfates from acid sulfate waters, Rev. Mineral. Geochem., 40, 351–403, 2000.

Brese, N. E. and O'Keeffe, M.: Bond-valence parameters for solids, Acta Crystallogr. B, 47, 192–197, 1991.

Bruker AXS Inc.: APEX4, Bruker Advanced X–ray Solutions, Madison, Wisconsin, USA, 2022.

Casey, W. H.: Large aqueous aluminum hydroxide molecules, Chem. Rev., 106, 1–16, 2006.

Casey, W. H., Olmstead, M. M., and Phillips, B. L.: A new aluminum hydroxide octamer, $[Al_8(OH)_{14}(H_2O)_{18}](SO_4)_5 \cdot 16H_2O$, Inorg. Chem., 44, 4888–4890, 2005.

Čech, F.: Rostite, a new name for orthorhombic $Al(SO_4)(OH) \cdot 5H_2O$, N. Jb. Miner., Mh., 1979, 193–196, 1979.

Čejka, J., Sejkora, J., Plášil, J., Bahfenne, S., Palmer, S. J., and Frost, R. L.: A vibrational spectroscopic study of hydrated Fe^{3+} hydroxyl-sulfates; polymorphic minerals butlerite and parabutlerite, Spectrochim. Acta A., 79, 1356–1363, 2011.

Chou, I.-M., Seal II, R. R., and Wang, A.: The stability of sulfate and hydrated sulfate minerals near ambient conditions and their significance in environmental and planetary sciences, J. Asian Earth Sci., 62, 734–758, 2013.

Chukanov, N. V., Aksenov, S. M., Rastsvetaeva, R. K., Kampf, A. R., Möhn, G., Belakovskiy, D. I., and Lorenz, J. A.: Riotintoite, $Al(SO_4)(OH) \cdot 3H_2O$, a new mineral from La Vendida copper mine, Antofagasta region, Chile, Can. Mineral., 54, 1293–1305, 2016.

Clayton, T.: Hydrobasaluminite and basaluminite from Chickerell, Dorset, Mineral. Mag., 43, 931–937, 1980.

Dahmen, T. and Gruehn, R.: Beiträge zum thermischen Verhalten von Sulfaten, IX. Einkristallstrukturverfeinerung der Metall(III)-sulfate $Cr_2(SO_4)_3$ und $Al_2(SO_4)_3$, Z. Kristallogr., 204, 57–65, 1993.

de Bruyin, H., Schoch, A. E., Beukes, G. J., Bok, L. D. C., and van der Westhuizen, W. A.: Note on cell parameters of zaherite, Mineral. Mag., 49, 145–146, 1985.

Dini, A.: Ore deposits, industrial minerals and geothermal resources, Per. Mineral., 72, 41–52, 2003.

Fang, J. H. and Robinson, P. D.: Alunogen, $Al_2(H_2O)_{12}(SO_4)_3 \cdot 5H_2O$: Its atomic arrangement and water content, Am. Mineral., 61, 311–317, 1976.

Farkas, L. and Pertlik, F.: Crystal structure determinations of felsőbányaite and basaluminite, $Al_4(SO_4)(OH)_{10} \cdot 4H_2O$, Acta Mineral. Petrogr., 38, 5–15, 1997.

Farkas, L. and Werner, P.-E.: Powder diffraction studies on aluminite and meta-aluminite, Z. Kristallogr., 151, 141–152, 1980.

Ferraris G. and Franchini-Angela, M.: Survey of the geometry and environment of water molecules in crystalline hydrates studied by neutron diffraction, Acta Crystallogr. B, 28, 3572–3583, 1972.

Ferraris, G. and Ivaldi, G.: Bond valence vs bond length in O···O hydrogen bonds, Acta Crystallogr. B, 44, 341–344, 1988.

Frondel, C.: Meta-aluminite, a new mineral from Temple Mountain, Utah, Am. Mineral., 53, 717–721, 1968.

Gamyanin, G. M., Zhdanov, Y. Y., Zayakina, N. V., Gamyanina, V. F., and Suknev, V. S.: Mangazeite, $Al_2(SO_4)(OH)_4 \cdot 3H_2O$ – a new mineral, Zap. Ross. Mineral. Obsh., 135, 20–24, 2006 (in Russian).

Hawthorne, F. C.: Towards a structural classification of minerals: the $^{vi}M^{iv}T_2\emptyset_n$ minerals, Am. Mineral., 70, 455–473, 1985.

Hawthorne, F. C., Krivovichev, S. V., and Burns, P. C.: The crystal chemistry of sulfate minerals, Rev. Mineral. Geochem., 40, 1–112, 2000.

Kahlenberg, V., Braun, D. E., Krüger, H., Schmidmair, D., and Orlova, M.: Temperature- and moisture-dependent studies on alunogen and the crystal structure of meta-alunogen determined from laboratory powder diffraction data, Phys. Chem. Mineral., 44, 95–107, 2017.

Kampf, A. R., Cooper, M. A., Hughes, J. M., Nash, B. P., Hawthorne, F. C., and Marty, J.: Caseyite, a new mineral containing a variant of the flat-Al_{13} polyoxometalate cation, Am. Mineral., 105, 123–131, 2020.

Kampf, A. R., Cooper, M. A., Hughes, J. M., Ma, C., Casey, W. H., Hawthorne, F. C., and Marty, J.: Protocaseyite, a new decavanate mineral containing a $[Al_4(OH)_6(H_2O)_{12}]^{6+}$ linear tetramer, a novel isopolycation, Am. Mineral., 107, 1181–1189, 2022.

Krivovichev, S. V.: Polyoxometalate clusters in minerals: review and complexity analysis, Acta Crystallogr. B, 76, 618–629, 2020.

Lattanzi, P.: Epithermal precious metal deposits of Italy – an overview, Miner. Dep., 34, 630–638, 1999.

Lepore, G. O., Bindi, L., Di Benedetto, F., Mugnaioli, E., Viti, C., Zanetti, A., Ciriotti, M. E., and Bonazzi, P.: A multimethodic approach for the characterization of manganiceladonite, a new member of the celadonite family from Cerchiara mine, Eastern Liguria, Italy, Mineral. Mag., 81, 167–173, 2017.

Libowitzky, E.: Correlation of O–H stretching frequencies and O–H···O hydrogen bond lengths in minerals, Monat. Chem., 130, 1047–1059, 1999.

Manasse, E.: Melanteria e fibroferrite delle Cetine (Siena), Atti Soc. Tosc. Sci. Nat., Proc. Verb., 17, 51–56, 1908.

Mandarino, J. A.: The Gladstone-Dale relationship, Part III. Some general applications, Can. Mineral., 17, 71–76, 1979.

Mandarino, J. A.: The Gladstone-Dale relationship, Part IV. The compatibility concept and some application, Can. Mineral., 19, 441–450, 1981.

Martin, R., Rodgers, K. A., and Browne, P. R. L.: The nature and significance of sulphate-rich, aluminous efflorescences from the Te Kopia geothermal field, Taupo Volcanic Zone, New Zealand, Mineral. Mag., 63, 413–419, 1999.

Mauro, D. and Biagioni, C.: New crystal-structure data on bohuslavite, $Fe^{3+}(PO_4)_3(SO_4)(OH)(H_2O)_{10} \cdot nH_2O$, Minerals, 13, 286, https://doi.org/10.3390/min13020286, 2023.

Mauro, D., Biagioni, C., Bonaccorsi, E., Hålenius, U., Pasero, M., Skogby, H., Zaccarini, F., Sejkora, J., Plášil, J., Kampf, A.R., Filip, J., Novotný, P., Škoda, R., and Witzke, T.: Bohuslavite, $Fe^{3+}(PO_4)_3(SO_4)(OH)(H_2O)_{10} \cdot nH_2O$, a new hydrated iron phosphate-sulfate, Eur. J. Mineral., 31, 1033–1046, 2019.

Mauro, D., Biagioni, C., Pasero, M., and Zaccarini, F.: Crystal-chemistry of sulfates from the Apuan Alps, Tuscany, Italy. VIII. New data on khademite, $Al(SO_4)F(H_2O)_5$, Mineral. Mag., 84, 540–546, 2020.

Menchetti, S. and Sabelli, C.: Alunogen. Its structure and twinning, Tschermaks Mineral. Petrogr. Mitt., 21, 164–178, 1974.

Menchetti, S. and Batoni, M.: Le Cetine di Cotorniano, Miniera & Minerali. Associazione Micro-mineralogica Italiana, Cremona, 353 pp., ISBN 978-88-905541-3-1, 2015.

Myneni, S. C.: X-ray and vibrational spectroscopy of sulfate in earth materials, Rev. Mineral. Geochem., 40, 113–172, 2020.

Nakamoto, K.: Infrared and Raman spectra of inorganic and coordination compounds Part A: Theory and application in inorganic chemistry, John Wiley and Sons, Hoboken New Jersey, 419 pp., https://doi.org/10.1002/9780470405840, 2009.

Olmi, F. and Sabelli, C.: Brizziite, $NaSbO_3$, a new mineral from the Cetine mine (Tuscany, Italy): description and crystal structure, Eur. J. Mineral., 6, 667–672, 1994.

Olmi, F., Sabelli, C., and Trosti-Ferroni, R.: Rosenbergite, $AlF[F_{0.5}(H_2O)_{0.5}]_4 \cdot H_2O$, a new mineral from the Cetine mine (Tuscany, Italy): description and crystal structure, Eur. J. Mineral., 5, 1167–1174, 1993.

Panichi, U.: Millosevichite, nuovo minerale del Faraglione di Levante nell'Isola di Vulcano, Rend. Accad. Naz. Lincei Cl. Sci. Fis. Mat. Nat., 22, 303–303, 1913.

Perkins, C. K., Eitrheim, E. S., Fulton, B. L., Fullmer, L. B., Colla, C. A., Park, D. H., Oliveri, A. F., Hutchison, J. E., Nyman, M., Casey, W. H., Forbes, T. Z., Johnson, D. W., and Keszler, D. A.: Synthesis of an aluminum hydroxide octamer through a simple dissolution method, Ang. Chem., 56, 10161–10164, 2017.

Pouchou, J. L. and Pichoir, F.: "PAP" ($\varphi\rho Z$) procedure for improved quantitative microanalysis, in: Microbeam Analysis, edited by: Armstrong, J. T., San Francisco Press, San Francisco, 104–106, 1985.

Sabelli, C.: I minerali delle Cetine di Cotorniano (SI): i solfati dimorfi jurbanite e rostite, Per. Mineral., 53, 53–65, 1984.

Sabelli, C.: Refinement of the crystal structure of jurbanite, $Al(SO_4)(OH) \cdot 5H_2O$, Z. Kristallogr., 173, 33–39, 1985a.

Sabelli, C.: Uklonskovite, $NaMg(SO_4)F \cdot 2H_2O$: new mineralogical data and structure refinement, Bull. Minéral., 108, 133–138, 1985b.

Sabelli, C. and Brizzi, G.: Alteration minerals of the Cetine mine, Tuscany, Italy, Mineral. Rec., 15, 27–36, 1984.

Sabelli, C. and Santucci, A.: Rare sulfates from the Cetine mine, Tuscany, Italy, N. Jb. Miner., Mt., 1987, 171–182, 1987.

Sabelli, C. and Trosti Ferroni, R.: The crystal structure of aluminite, Acta Crystallogr. B, 34, 2407–2412, 1978.

Sabelli, C. and Vezzalini, G.: Cetineite, a new antimony oxide-sulfide mineral from Cetine mine, Tuscany, Italy, N. Jb. Miner. Mh., 1987, 419–425, 1987.

Schindler, M. and Hawthorne, F. C.: A bond-valence approach to the structure, chemistry and paragenesis of hydroxy-hydrated oxysalt minerals, I. Theory, Can. Mineral., 39, 1225–1242, 2001.

Schmetzer, K., Ottemann, J., and Bank, H.: Schlossmacherit, $(H_3O,Ca)Al_3[(OH)_6|((S,As)O_4)_2]$, ein neues Mineral der Alunit-Jarosit Reihe, N. Jb. Miner., Mh., 1980, 215–222, 1980.

Seichter, W., Moegel, H. J., Brand, P., and Salah, D.: Crystal structure and formation of the aluminum hydroxide chloride $[Al_{13}(OH)_{24}(H_2O)_{24}]Cl_{15} \times 13H_2O$, Eur. J. Inorg. Chem., 1998, 795–797, 1998.

Sheldrick, G. M.: Crystal structure refinement with SHELXL, Acta Crystallogr. C, 71, 3–8, 2015.

Sillitoe, R. H. and Brogi, A.: Geothermal systems in Northern Apennines, Italy: modern analogues of Carlin-style gold deposits, Econ. Geol., 116, 1491–1501, 2021.

Smith, D. G. W. and Nickel, E. H.: A system for codification for unnamed minerals: report of the Subcommittee for Unnamed Minerals of the IMA Commission on New Minerals, Nomenclature and Classification, Can. Mineral., 45, 983–1055, 2007.

Wilson, A. J. C. (Ed.): International Tables for Crystallography Volume C: Mathematical, Physical and Chemical Tables, Kluwer Academic Publishers, Dordrecht, the Netherlands, 1992.

Wright, F. E.: Computation of the optic axial angle from the three principal refractive indices, Am. Mineral., 36, 543–556, 1951.

Zimbelman, D. R., Rye, R. O., and Breit, G. N.: Origin of secondary sulfate minerals on active andesitic stratovolcanoes, Chem. Geol., 215, 37–60, 2005.